PNAS
www.pnas.org

Supplementary Information for

Intrinsic mutant HTT-mediated defects in oligodendroglia cause myelination deficits and behavioural abnormalities in Huntington disease

Costanza Ferrari Bardile, Marta Garcia-Miralles, Nicholas S. Caron, Nirmala Arul Rayan, Sarah R. Langley, Nathan Harmston, Ana Maria Rondelli, Roy Tang Yi Teo, Sabine Waltl, Lisa M. Anderson, Han-Gyu Bae, Sangyong Jung, Anna Williams, Shyam Prabhakar, Enrico Petretto, Michael R. Hayden, Mahmoud A. Pouladi

Corresponding author: Dr. Mahmoud A. Pouladi
Email: pouladi@tlgm.a-star.edu.sg; map@pouladilab.org

This PDF file includes:

Supplementary Materials and Methods
Figs. S1 to S6
Tables S1 to S3
Captions for Datasets S1 to S3
References for SI reference citations

Other supplementary materials for this manuscript include the following:

Datasets S1 to S3

Supplementary Materials and Methods

Animals

Mice were housed in individually ventilated cages with littermates of mixed genotype (2-5 per cage) and maintained on a reverse 12-h light/dark cycle (lights on at 09:00) with free access to water and food (Altromin 1324 irradiated modified 18 % Protein and 6 % Fat) throughout the study. Mice were maintained under standard conditions and all animal procedures were performed with the approval of the Institutional Animal Care and Use Committee (IACUC # 151067) at Biological Resource Centre (BRC), A*STAR and in accordance with their approved guidelines.

Real-time quantitative PCR

Total RNA from OPCs was extracted from a minimum of two pooled pup cortices per independent biological replicate using the PureLink RNA Micro Kit (Invitrogen). First-strand cDNA synthesis was performed using the SuperScript First Strand Synthesis System (Invitrogen). Expression of human full-length (FL) mHTT was analysed by qPCR, running each sample in triplicate with Sybr Select Universal Master Mix (Invitrogen) on a StepOnePlus to obtain Ct values. The human-specific primers for mHTT and the mouse-specific primers for beta-actin are summarized in Table S3.

Transmission electron microscopy

Brain samples were sent to the Harvard Medical School EM unit for further processing. Briefly, coronal slices at the level of Bregma -1 mm were made from the central part of the corpus callosum before post-fixation in 1% osmium tetroxide/1.5% potassium ferrocyanide solution for 1 h. After washing with 1% uranyl acetate in maleate buffer, the samples were dehydrated, infiltrated with epon, embedded, and polymerised at 60°C for two days. Ultra-thin slices (100 nm) were cut before imaging on a transmission electron microscope. For image analyses, axon and myelin fibres diameters were measured using ImageJ. A number of 3-4 animals per genotype was used and more than 300 axons were analysed for each mouse. G-ratios were calculated within equal axonal distributions (Fig. S6A-B).

Corpora callosa slice preparation and electrophysiology

The ACSF cutting solution used was: 206 mM Sucrose, 2 mM KCl, 1.25 mM NaH2PO4, 26 mM NaHCO3, 10 mM Glucose, 2 mM MgCl2, 2 mM MgSO4, 1 mM CaCl2. The osmolarity of the solution was adjusted to 305-315 mOsm and the pH to 7.3-7.4 with HCl. 450 μm coronal slices were cut with a Vibratome (Leica VT1200s) at a speed of 0.3 mm/sec with frequency set at 1 mm. Brain slices were transferred to a holding chamber filled with oxygenated (95% O_2 + 5% CO_2) standard ACSF solution (124 mM NaCl, 2.5 mM KCl, 1.2 mM NaH_2PO_4, 24 mM $NaHCO_3$, 5 mM HEPES, 12.5 mM Glucose, 2 mM $MgSO_4$, 2 mM CaCl) at 37°C for 30 minutes, following other 30 minutes at RT before starting the recording.

Compound action potentials (CAPs) evoked by stimulation were recorded in the corpora callosa at 3 different distances: 1.5 mm, 1 mm and 0.5 mm distance. The recording electrode pipette (1.5-3 MΩ) filled with 3M NaCl was first placed 1.5 mm away from the midline of brain slice, and stimulation electrode was placed 0.5 mm away from middle line on the opposite side of recording pipette. The intensity of the stimulus was increased from 0.1 mA to 5 mA with 0.5 mA of steps using external stimulator (model 2100, A-M system), and responses were recorded at each step in triplicate. The Multiclamp 700B was used for recordings, Digidata 1550B and pClamp10 software (Molecular Device). From obtained data, amplitudes, area of N1 (myelinated) and N2 (non-myelinated) were calculated using Population spike analysis tool in AxoGraph X (AxoGraph Scientific). The averaged maximum amplitude in each group was fitted as function of the current intensities. The maximum area of peaks from 5 mA of stimulation were used to compare between groups. Duration of peaks were measured by latency from starting point and ending point of peak on Axograph X, and the duration from the maximum slice were used to compare between groups. Wilcoxon sign rank test was used to compare the difference between groups due to small sample size (WT, n=3; BACHD, n=3; BN, n=4).

Behavioural test of affective function

A longitudinal design was used to evaluate the phenotype at different ages and the same mice were followed for all tests. Mice were habituated to the testing room for 30 min previous each behavioural test. Investigator was blinded for all the tests and a different investigator analysed the data.

Rotarod test of motor learning and motor coordination. The rotarod test is classically used to evaluate motor function in rodents. Training was performed at 2 months of age. Testing was performed every 2 months between 2 and 12 months of age. Motor learning, and motor coordination and balance were assessed using accelerating rotarod tasks (UGO Basile 47600 Rotarod, rotating rod diameter 3 cm). For training, three trials (120 s) per day at a fixed-speed of 18 rpm for three consecutive days were given. For the testing phase, three trials (5 min) in acceleration from 5 to 40 rpm were given. Rotarod scores are the average of three trials spaced 2 h apart.

Climbing test. The climbing test is used to monitor motor impairments in rodents (1). Testing was performed every 2 months between 2 and 12 months of age. Mice were placed under a metal wire mesh cylinder (10.5 cm of diameter, 15.5 cm high, open at bottom end) for 6 min. The test sessions were recorded by video camera and the latency to climb and the total time spent climbing were scored blinded. Climbing was determined when all four paws of the mouse were on the walls of the cylinder. Time spent climbing is taken as a measure of motor function.

Open-field test of anxiety. The open field test is classically used to assess anxiety in rodents (2). The test is based on the natural conflict between the tendency of mice to explore a novel environment and the aversive properties of open and bright spaces. The testing apparatus is a 50 × 50 cm open, grey, acrylic box (open field) with 20-cm high walls. Time spent in the center versus the perimeter is taken as a measure of anxiety-like

behaviour. Mice were placed individually in the center of the open field for 10 min and the time spent in the center versus perimeter were recorded using an automated video-based tracking system (Noldus EthoVision 9, Netherlands).

Porsolt forced swim test (FST) of depression. The Porsolt FST is used to test for depressive-like behaviour in rodents. The test is based on the assumption that an animal will try to escape an aversive and stressful stimulus. The test was performed at 12 months of age as previously described (3). Briefly, mice were placed in individual cylinders (25 cm tall x 19 cm wide) filled with room temperature water (23-25^{o}C) to a depth of 15 cm for a period of 6 min. The test sessions were recorded and examined blinded. The last 4 min of the test session was scored using a time-sampling technique to rate the predominant behaviour over 5-sec intervals. The following behaviours were measured and recorded at the end of every 5 sec: swimming/climbing and immobility. Time spent immobile is taken as a measure of depressive-like behaviour.

Simple test of swimming ability. To determine whether the ability to swim is comparable among the different genotypes, a simple swimming ability test was performed. Mice were placed at the end of one arm of a T maze while the main arm was closed in order to make the mice swimming in a linear chamber (88 x 10 cm; water depth, 11 cm). Mice had to reach a platform (8 x 10 cm) on the other end of the chamber to escape from the water. Swimming time was measured with three consecutive trials for each mouse.

Immunohistochemistry and stereological measurements

Perfused brains were post-fixed overnight in 4% PFA before switching to 30% sucrose in 1xPBS. Brains were cut via cryostat (Leica CM3050S) into a series of 25µm coronal sections free- floating in PBS with 0.01% sodium azide. For BrdU staining, antigen retrieval was necessary. Sections were pretreated with 1 N HCl (pre-cool wells) for 10 minutes shaking on ice, before moving into 2 N HCl shaking at room temperature (RT) for an additional 10 minutes. Sections were subsequently put at 37^{o}C (pre-warmed wells) shaking in the water bath for 20 minutes, followed by neutralization with 0.1M borate buffer at pH 9 shaking at RT for 10 minutes. For all stainings, sections were washed 3 times with 1 x phosphate buffered saline (PBS), then sections were blocked in 5% normal goat serum (NGS) in PBS containing 0.1% Triton X-100 (TX) for 120 minutes at RT. Sections were then incubated with primary antibodies in 1% NGS in PBS-TX overnight at RT. Rabbit anti-Olig2 at 1:750 (Chemicon AB9610), rabbit anti-GSTpi at 1:2000 (MBL, 311), goat anti-PDGFRα at 1:300 (R&D Systems, Cat# AF1062) and rat anti-BrdU at 1:500 (ABD serotec OBT0030) were used. Sections were washed 3 times with PBS and incubated with secondary antibodies at 1:500 (Life Technologies A11008 and A11077) in PBS-Tx at RT for 2hrs. 12 sections spaced 200 µm apart and spanning the region of interest were mounted and 3 sections from each animal were analysed. Briefly, corpus callosum, striatum and subventricular zone from one hemisphere were traced using the Stereo Investigator software (MBF Bioscience) and Olig2 positive (+), GSTpi positive (+), PDGFRα positive (+) and Olig2+/BrdU+ cells were counted in the entire region of interest.

For stereological measurements of the striatum, a series of sections spaced 200 μm apart and spanning the striatum were stained for NeuN (1:1000, Millipore) using biotinylated anti-mouse secondary antibody (1:1000, Vector Laboratories), the ABC Elite Kit (Vector) to amplify signal, and 3,3'-diaminobenzidine (DAB, Thermo Scientific) detection. Structures were traced using Stereo Investigator software (MBF Bioscience) and volumes determined using the Cavalieri principle.

Protein analysis

For H3 and H3K27e3, protein lysates were sonicated for 2 cycles of 30 sec on, 30 sec off. 70 μg of protein lysates for H3 and H3K27me3, and 30 μg for the rest of the proteins were separated on 12% Bis-Tris protein gel (Novex) with 20X MES running buffer (Novex) and transferred on nitrocellulose membranes. The following primary antibodies were used: H3 (1:1000, Cell Signaling, cat no. 4499), H3K27me3 (1:1000, Merck, cat no. 07-449), Ermin (1:1000; Merck, cat. no. MABN323), MBP (1:500; Millipore, cat. no.MAB386), MAG (1:2000; Millipore, cat. no. MAB1567) and Calnexin (1:5000; Sigma-Aldrich, cat. no. C4731). Primary antibodies were incubated at 4°C overnight. Secondary antibodies (1:10,000) were used: Alexa-Fluor goat anti-rabbit 800, Alexa-Fluor goat anti-mouse 680, Alexa-Fluor goat anti-rabbit 680 and Alexa-Fluor goat anti-rat 800 (all from Life Technologies). The membrane was imaged using the LiCor Imaging System and Odyssey V3.0 software (LiCor), followed by intensity analysis with ImageJ.

RNA-seq analysis

Subsequent library preparation and paired-end 150bp sequencing and 15M reads/per sample using HiSeq were performed by Novogene (Hong Kong). The data quality of the Fastq files was assessed using FastQC (4). The reads were aligned to the mm10 genome (Ensembl version 85) using STAR 2.5.2a (5) and quantified using RSEM 1.2.30(6). Differential expression was calculated with DESeq2 (7) using tximport (35). Mitochondrial and ribosomal genes were removed from further analysis to avoid confounding technical factors (e.g. differences in poly-A capture/Ribo-Zero rRNA removal efficiencies and the number of mitochondria between samples). Significant differential expression was calculated using the Wald test when comparing between two conditions and with the likelihood ratio test when comparing across all three conditions. Hierarchical clustering and bootstrapping was performed with the pvclust R package (8). The significantly different clusters were identified using 10,000 bootstraps and the Approximately Unbiased (AU) and Bootstrap Probability (BP) p-values were calculated. For AU/BP p-values greater than 0.95, one can reject the hypothesis that the cluster does not exist with a significance level of 0.05, therefore we deemed sets of samples with AU/BP p-values greater than 0.95 to be significantly clustered. Differences in gene expression were significant at a BH-corrected 10% false-discovery rate (FDR) level. Functional enrichment was calculated using gProfileR at a 5% FDR, excluding IEA terms (9) with the background set to all expressed genes. Sequencing reads have been deposited into SRA with accession number SRP143632. RNA-sequencing data of murine oligodendroglia differentiation was downloaded from GEO (GSE52564, (10)).

Transcripts per million (TPM) values were calculated from the provided FPKM values. De novo motif discovery was performed using HOMER (11) using the list of up-regulated genes in BN versus BACHD was used for this analysis. Transcription factor changes were identified using the ChIP-seq/chip Enrichment Analysis (ChEA) tool and database (12). The entire list of DEGs identified between BACHD and BN mice was used for this analysis.

ChIP-seq analysis

Dissected tissues were mechanically dissociated by passing through a cell strainer and fixed in 1% formaldehyde (diluted from 37% stock solution, Sigma, F8775). Cell membrane and nuclei were lysed sequentially and resuspended in SDS buffer. The nuclei were sonicated for 500 cycles/bursts with Covaris sonicator (Covaris). Following sonication, samples were diluted with IP dilution buffer and incubated with 3µl of anti-EZH2 (D2C9, Cell Signaling) and anti-SUZ12 antibodies (D39F6, Cell Signaling). Following washing, chromatin was reverse-crosslinked for purification of DNA. NGS libraries were constructed using the purified ChIP DNA using Illumina Truseq DNA library prep kit (Illumina Cat.no. FC-121-2003). Libraries were multiplexed and sequenced on HiSeq4K Illumina platform as paired end 76 basepair reads. ChIP-seq reads were aligned to the mouse genome (mm10) using bwa (37), duplicate reads were filtered using samblaster (38). Quality control of ChIP-sequencing data was performed using ChIPQC (39). Peaks were called using MACS2 (40), with an FDR < 10%. The overlap between SUZ12 and EZH2 peaks was performed by resizing each peak to be 500bp around its midpoint and significance of overlap calculated using the hypergeometric test from the ChIPpeakAnno (41) package, using 10% as the bindable fraction of the genome. Genes which had at least one annotated TSS +/- 5kb overlapping a peak were designated as bound by a factor in a specific experimental condition. ChIP-seq data was visualised using the Gviz package. Differential binding analysis was performed using diffReps (42), using a G-test. Differentially bound peaks were defined as those which overlapped a window reported by diffReps as significantly different bound (FDR < 5%) in at least one comparison. Ontology enrichment analysis of differentially bound peaks was performed using GREAT (43). Terms which were identified as having FDR < 5% for both the binomial and hypergeometric tests and a region-level fold-enrichment > 2 were defined as significant.

Data availability

The RNA-seq and ChIP-seq sequencing data supporting the findings of this study have been deposited into SRA with accession number SRP143632 and SRP159123, respectively.

Statistical analysis

Prism 6 (GraphPad Software) was used for statistical analyses and data are expressed as means ± SEM. When only two experimental groups were compared, the Student's t-test was used to calculate statistical significance. Regression analysis was used to examine

the correlation between body weight and performance in select behavioural tests. Chi-square test was used to calculate enrichment of EZH2 binding in the promoters of differentially expressed genes. Unless otherwise stated, for all other experiments statistical significance was calculated using one-way ANOVA or two-way ANOVA, followed by Tukey's multiple comparisons test. Differences were considered statistically significant when $P < 0.05$ unless an otherwise stated FDR correction was applied. R/Bioconductor was used for RNA-seq and ChIP-seq analyses.

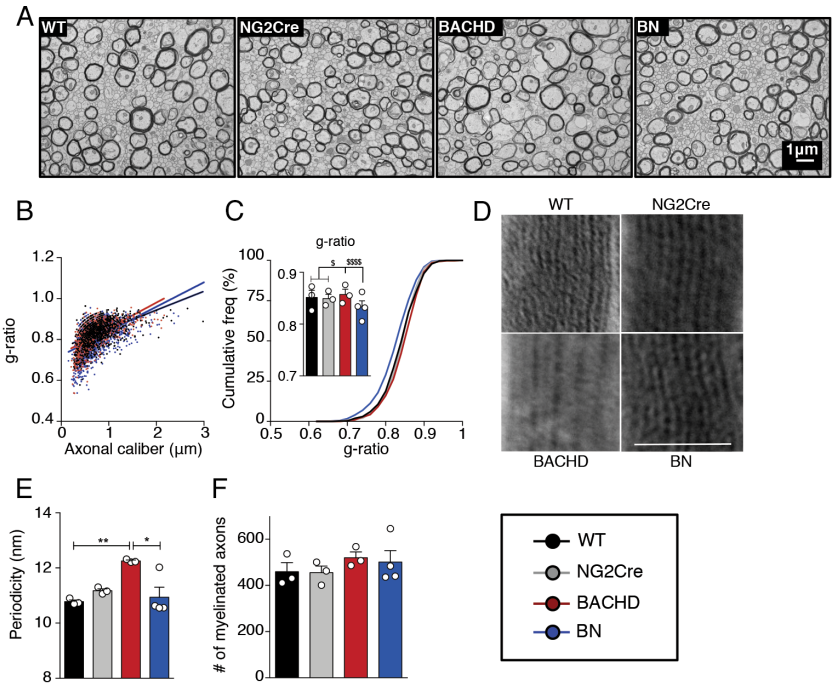

Fig. S1. OPC-intrinsic effects of mHTT cause myelin thinning in HD mice at early age. (A) EM images of myelinated axons in the corpus callosum at 1 month of age. Scale bar represents 1 µm. (B,C) Higher g-ratios (thinner myelin sheaths) in BACHD mice are rescued in BN mice. (D) Representative images of myelin sheath layers. (E) Higher periodicity in BACHD mice (less compactness in myelin sheath) is rescued in BN mice. (F) Number of myelinated axons is the same among genotypes. N = 3-4 per genotype; ~300 axons analyzed per animal. Data are mean ± SEM; * $P < 0.05$, ** $P < 0.01$ by one-way ANOVA followed by Tukey's test in E. For *C and F*, $P > 0.05$ by one-way ANOVA, statistical comparison shown represents two-tailed unpaired Student's t-test, \$ $P < 0.05$, \$\$\$\$ $P < 0.001$.

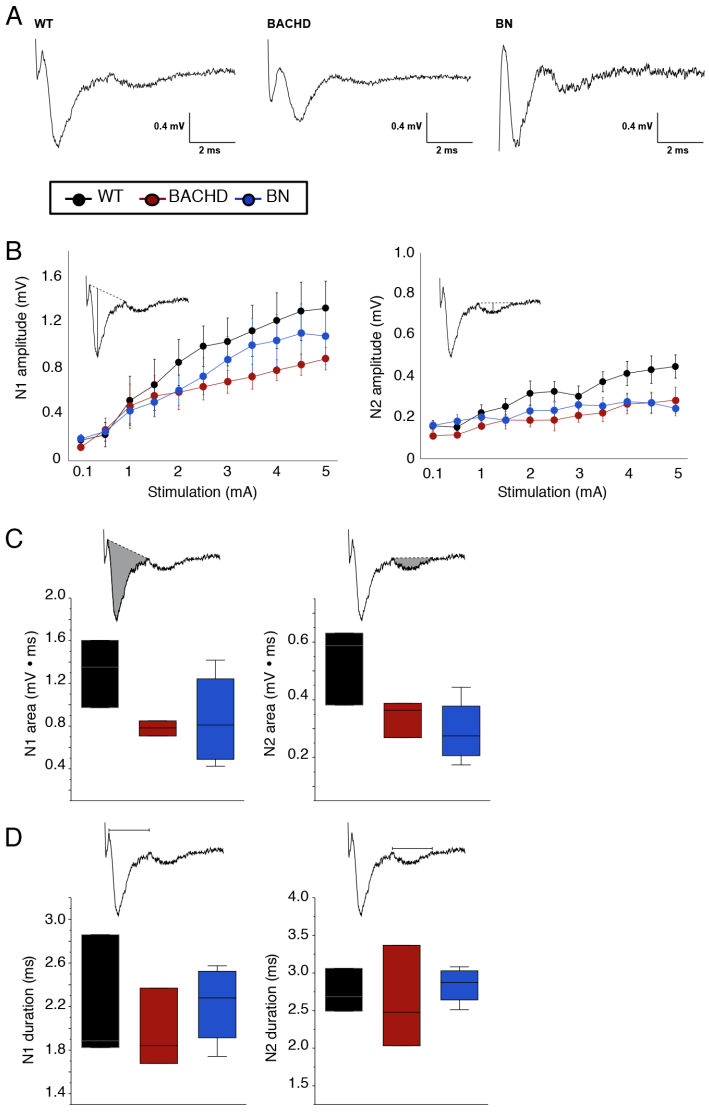

Fig. S2. OPC-intrinsic effects of mHTT on compound action potential of myelinated and unmyelinated fibers. (A) Representative CAP traces evoked by 5 mA stimulus in WT, BACHD and BN corpora callosa. (B) CAPs evoked by increasing stimulation strength for myelinated (N1) and unmyelinated (N2) fibers show decreased action potential transmission in BACHD myelinated axons, although not statistically significant. (C) Decreased area of CAPs were detected on BACHD and BN, but not significant in both N1 (WT/BACHD, *P*=0.10; BACHD/BN, *P*=0.40; WT/BN, *P*=1.00) and N2 (WT/BACHD, *P*=0.20; BACHD/BN, *P*=0.11; WT/BN, *P*=0.63). (D) Duration of CAPs was comparable between groups in both N1 (WT/BACHD, *P*=0.70; BACHD/BN, *P*=1.00; WT/BN, *P*=0.40) and N2 (WT/BACHD, *P*=0.70; BACHD/BN, *P*=0.63; WT/BN, *P*=0.63). Data show means ± SEM. Wilcoxon sign rank test was used to calculate statistical significance due to small size of sample (3-4 per genotype).

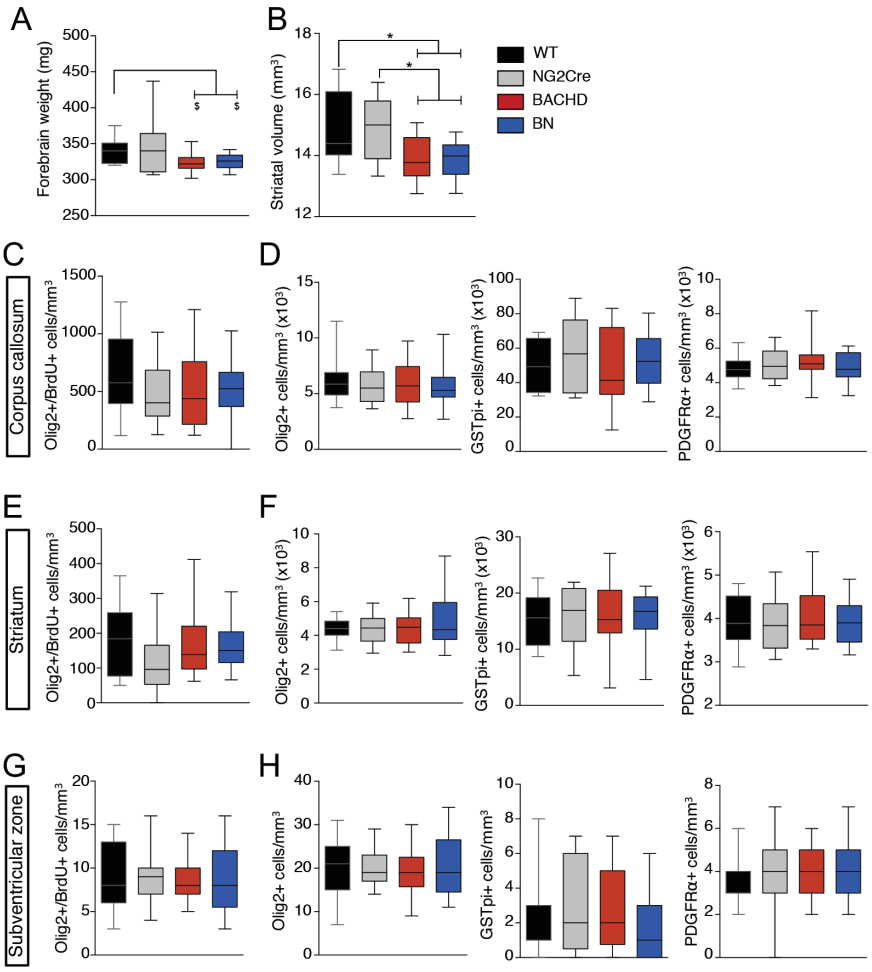

Fig. S3. Absence of OPC-intrinsic effects of mHTT on neuropathology and oligodendrogenesis in HD mice. (A,B) Forebrain weight and striatal volume were evaluated in 12 months old mice as measures of neuropathology. BACHD mice present significant deficits in (A) forebrain weight and (B) striatal volume compared with WT mice. Forebrain weight and striatal volume loss are not rescued in BN mice (A,B). (C,E,G) Proliferation of Olig2 and (D,F,H) density of Olig2, GST-pi and PDGFRα expressing cells in corpus callosum (C,D), striatum (E,F), and subventricular zone (G,H) show no differences among genotypes at 12 months of age. N = 13-18 per genotype. Data represent means ± SEM; * $P < 0.05$ or $^{\$}P < 0.05$; two-tailed unpaired Student's t-test in A (WT vs BACHD, $P = 0.0315$, t = 2.297, d.f. = 22; NG2Cre vs BACHD, $P = 0.0457$, t = 2.118, d.f. = 22; WT vs BN, $P = 0.0407$, t = 2.181, d.f .= 21) or one-way ANOVA followed by Tukey's test in B. Unpaired Student's t-test was used in A since any significant difference was reached with one-way ANOVA.

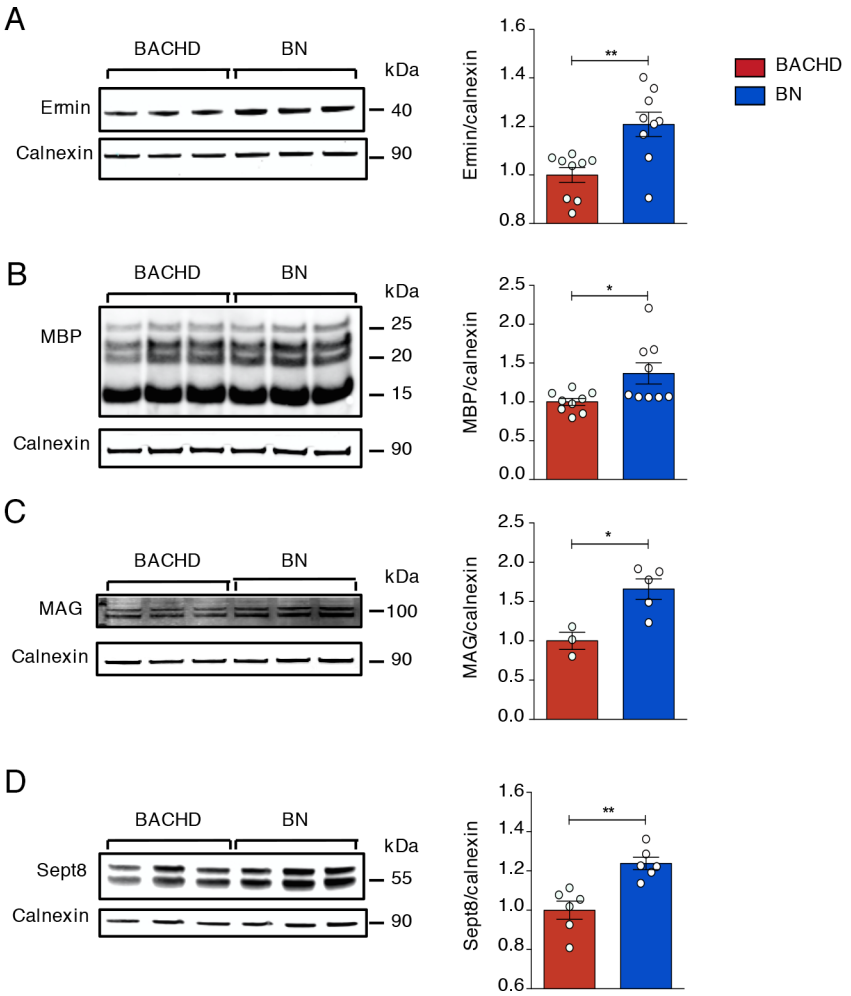

Fig. S4. Myelin protein expression in BACHD is mediated by OPC-intrinsic effects of mHTT. (A-D) BN mice present significant increase in (A) Ermin, (B) MBP, (C) MAG and (D) Septin-8 protein expression compared with BACHD mice in corpora callosa at 1 month of age. N = 9/genotype in A,B or N = 3-5 in C or N = 6 in D. All bands where used for quantification. Data represent means ± SEM; * $P < 0.05$, ** $P < 0.01$; two-tailed unpaired Student's test in A ($P = 0.0028$, t = 3.527, d.f .= 16), B ($P = 0.0206$, t = 2.569, d.f .= 16), C ($P = 0.0137$, t = 3.448, d.f .= 6), and D ($P = 0.0017$, t = 4.232, d.f .= 10).

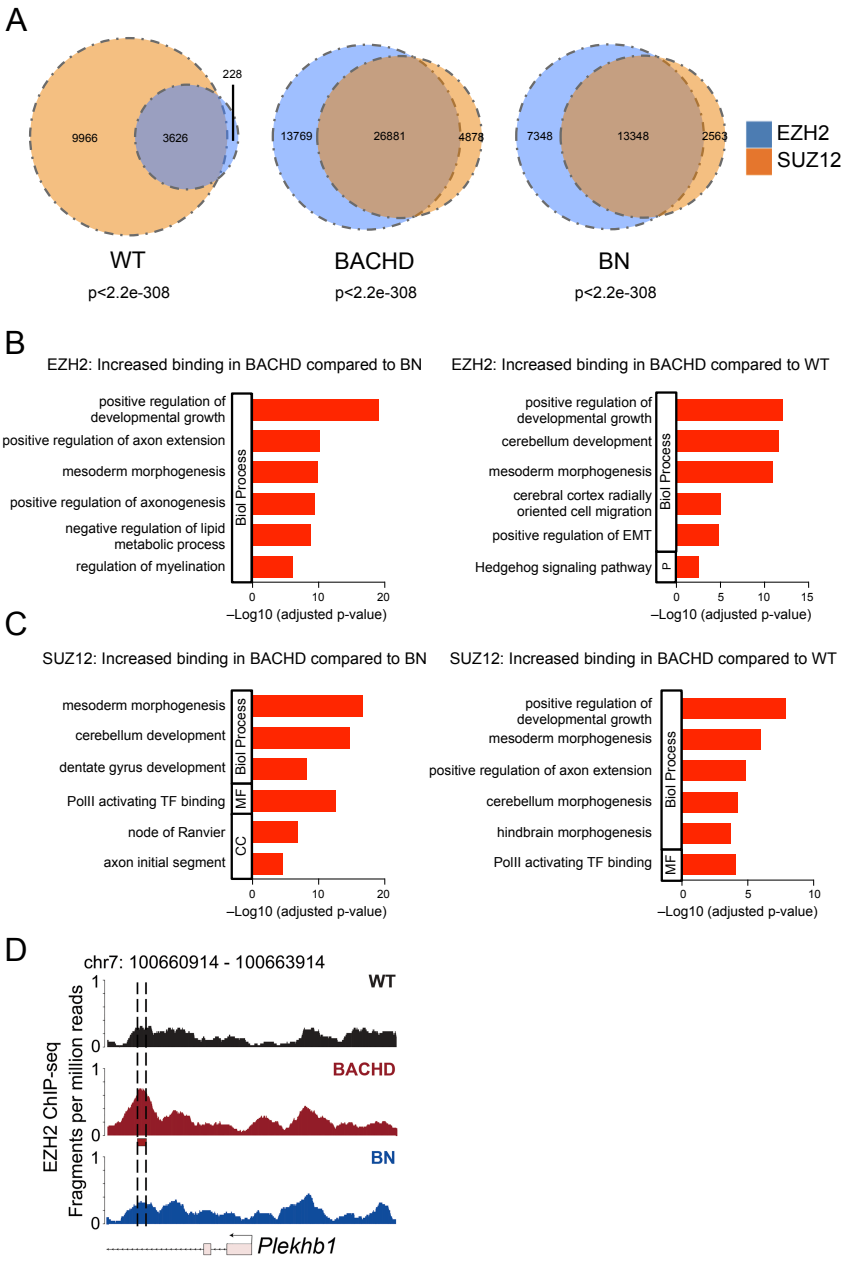

Fig. S5. EZH2 and SUZ12 binding site peaks overlap. (A) Venn diagram comparing EZH2 and SUZ12 binding site peaks show a significance overlap in the WT, BACHD, and BN conditions. (B-C) Ontology analysis generated using GREAT, reveals that binding events which are significantly increased in BACHD compared either to BN or WT, are enriched for processes directly related to neurogenesis, brain development and myelination. P = PANTHER pathway; EMT = epithelial to mesenchymal transition; PolII = RNA polymerase II; TF = transcription factor. (D) EZH2 binding in the proximity of the TSS of Plekhb1 is only observed in BACHD mice. This peak shows significantly higher binding in BACHD compared to BN (FDR < 0.02, log2FC = 0.52), while this region is not differentially bound between BN and WT (FDR=0.55, log2FC=0.29).

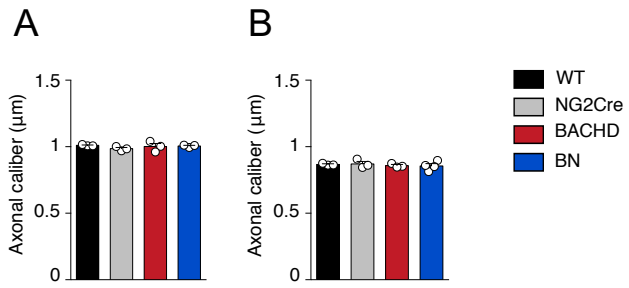

Fig. S6. Axonal caliber of analyzed axons. (A,B) Mean axonal caliber of analysed axons is equal among genotypes at 12 months (A) and 1 month of age (B). N = 3-4 per genotype; ~300 axons analyzed per animal. Data are mean ± SEM; P > 0.05 by one-way ANOVA followed by Tukey's test.

Table S1. ***De novo*** **sequence motifs found using HOMER analysis to be enriched in genes up-regulated in BN relative to BACHD mice.**

Motif	P-value	log P-value	Best Match
	1.00E-09	-2.29E+01	Nkx2-2
	1.00E-09	-2.29E+01	Tfap4
	1.00E-08	-1.85E+01	Zscan4
	1.00E-07	-1.82E+01	Nkx2-5
	1.00E-07	-1.81E+01	MafK
	1.00E-07	-1.67E+01	Zbtb7b
	1.00E-07	-1.66E+01	AR
	1.00E-06	-1.44E+01	INR
	1.00E-06	-1.39E+01	CREB
	1.00E-05	-1.24E+01	Zbtb7b
	1.00E-05	-1.19E+01	NHLH1
	1.00E-04	-1.12E+01	ZNF354C
	1.00E-03	-7.53E+00	Srf

Table S2: Primers used for PCR

Target	Forward primer (5'-3')	Reverse primer (5'-3')
loxP HTT exon1	ATTCATTGCCCCGTGCTGA	AGCCCTCTTCCCTCTCAGACTAGAAGAGG

Table S3: Primers used for cDNA analyses

Target	Forward primer (5'-3')	Reverse primer (5'-3')
Human mHTT	CAAGCCTTGCCGCATCAAAG	CCCCCTGTTAGCAAAAACGAA
Mouse beta-actin	GGCTGTATTCCCCTCCATCG	CCAGTTGGTAACAATGCCATGT

Additional Dataset S1 (separate file)
Differential Expression between WT, BN, and BACHD. The Excel spreadsheet provides gene names, gene IDs, log2 fold changes, p-values and adjusted p-values for genes differentially expressed between BN, BACHD and WT

Additional Dataset S2 (separate file)

Functional Enrichment Terms for Up-Regulated and Down-Regulated Genes. The Excel spreadsheet provides terms, term IDs, adjusted p-values and intersections of the functional enrichment terms for up-regulated and down-regulated genes between BN and BACHD.

Additional Dataset S3 (separate file)

Differential binding of EZH2 and SUZ12 in gene promoters (± 5kb from TSS). The Excel spreadsheet provides gene names, gene descriptions, gene IDs for increased and/or decreased EZH2 or SUZ12 binding in gene promoters in BN vs BACHD and BN vs WT.

Supplementary References

1. Garcia-Miralles M, et al. (2017) Early pridopidine treatment improves behavioral and transcriptional deficits in YAC128 Huntington disease mice. *JCI Insight* 2(23). doi:10.1172/jci.insight.95665.

2. Crawley JN (1985) Exploratory behavior models of anxiety in mice. *Neuroscience and biobehavioral reviews* 9(1):37–44.

3. Pouladi MA, et al. (2009) Prevention of depressive behaviour in the YAC128 mouse model of Huntington disease by mutation at residue 586 of huntingtin. *Brain* 132(Pt 4):919–932.

4. Andrews S (2010) FastQC: a quality control tool for high throughput sequence data.

5. Dobin A, et al. (2013) STAR: ultrafast universal RNA-seq aligner. *Bioinformatics* 29(1):15–21.

6. Li B, Dewey CN (2011) RSEM: accurate transcript quantification from RNA-Seq data with or without a reference genome. *BMC Bioinformatics* 12(1):323.

7. Love MI, Huber W, Anders S (2014) Moderated estimation of fold change and dispersion for RNA-seq data with DESeq2. *Genome biology* 15(12):550.

8. Suzuki R, Shimodaira H (2006) Pvclust: an R package for assessing the uncertainty in hierarchical clustering. *Bioinformatics* 22(12):1540–1542.

9. Reimand J, et al. (2016) g:Profiler-a web server for functional interpretation of gene lists (2016 update). *Nucleic Acids Research* 44(W1):W83–9.

10. Zhang Y, et al. (2014) An RNA-sequencing transcriptome and splicing database of glia, neurons, and vascular cells of the cerebral cortex. *J Neurosci* 34(36):11929–11947.

11. Heinz S, et al. (2010) Simple combinations of lineage-determining transcription factors prime cis-regulatory elements required for macrophage and B cell identities. *Mol Cell* 38(4):576–589.

12. Lachmann A, et al. (2010) ChEA: transcription factor regulation inferred from integrating genome-wide ChIP-X experiments. *Bioinformatics* 26(19):2438–2444.